ICAS 2021 SHANGHAI

32nd Congress
of the International Council
of the Aeronautical Sciences
September 6-10, 2021
Pudong Shangri-La, Shanghai, China

SOL-GEL BASED ORGANIC-INORGANIC HYBRID COATINGS FOR CORROSION PROTECTION OF AEROSPACE ALUMINIUM ALLOY

R. V. Lakshmi[1], S.T. Aruna[1], S. Sampath[2]

[1] Surface Engineering Division, CSIR - National Aerospace Laboratories, Bangalore-560017, India.
[2] Department of Inorganic and Physical chemistry, Indian Institute of Science, Bengaluru – 560012, India.

Abstract

Aluminum alloy 2024 is the most commonly used aircraft alloy because of its high damage tolerance, relatively high tensile strength and high strength to weight ratio. These properties are achieved by appropriate alloying with copper and magnesium which, in addition to strengthening phases, form copper- and magnesium-containing constituent particles. However, the presence of these alloying elements makes the alloy susceptible to localized corrosion making it impossible to use it without prior application of a corrosion protection system. Historically, the corrosion protection systems are based on Cr(VI) compounds which are now restricted due to their carcinogenic nature. In this direction, extensive research is pursued on organic–inorganic hybrid silane coatings to replace the toxic Cr (VI) component. In the present study, silica–alumina hybrid sol-gel coatings are developed and explored for anticorrosion properties using electrochemical techniques and industry-standard tests. Apart from the basic coating, corrosion inhibitors are explored to impart active protection to the alloy. The ability of silica-alumina coating to act as reservoir for storage of inhibitors is investigated. The results confirm that coatings containing cerium nitrate inhibitor in an optimum concentration offer superior protection to the surface. X-ray photoelectron and Raman spectroscopy studies provide evidence for the migration of cerium ions from the coating. Improved corrosion protection is attributed to the combined effect of the barrier nature of the coating and the corrosion inhibiting nature of Ce^{3+} ions. Further, the role of morphology of the inhibitor when used in the form of solid particles instead of salts is studied. The compatibility of the developed sol-gel layer with subsequent top layers of the paint system is also evaluated.

Keywords: AA 2024, corrosion, sol-gel, inhibitor, cerium.

1. Introduction

Among the many aluminium alloys that are used in aerospace industry, the quaternary Al–Cu–Mg–Mn 2024-T3 alloy is one of the most widely used alloy [1]. Aluminium alloy 2024 (AA 2024) possesses exceptionally high strength to weight ratio and damage-tolerance. It exhibits improved mechanical properties due to strengthening of the alloy matrix with several second-phase particles. Some phases however, are not desirable particularly from the point of corrosion resistance. AA 2024 is found to undergo localized corrosion by intergranular attack and pitting. To understand the corrosion process in this alloy, several studies have been carried out [2-8]. As per the understanding, overall corrosion on AA 2024 starts with dealloying of the anodic S-phase particle. The anodic reactions are basically the dealloying of Mg and Al that occur at the surface of the S-phase particles. The accompanying cathodic reactions, namely water reduction and oxygen reduction, most likely take place on the Al matrix at the periphery of the S-phase particles. Considerably high amount of OH^- ions gets generated from the coupled water and oxygen reduction reactions. Accordingly, a local alkalinity is formed around the S-phase remnant in a stagnant medium. Once the local pH exceeds 9 (i.e., equilibrium pH of Al oxide), the surrounding Al oxide layer are no longer stable and starts to dissolve (as per phase diagram of Al).

Corrosion activity on the AA 2024 surface is controlled either by providing passive protection or by active protection. Passive corrosion protection is provided by establishing a barrier on the surface such that the cathodic reaction is suppressed by limiting the diffusion of corroding agents, such as water and oxygen, to the aluminium surface. Generally, they are achieved by two methods; (a) Alcladding the alloy and (b) providing a corrosion inhibiting barrier coating. Often the barrier coating suppresses the penetration of corrosive electrolyte and prevents it from reaching the metal

surface. Existence of any minute flaws in the protective layer may lead to corrosion and propagation of pits. Thus, the barrier coatings as such are found to be inefficient to yield reliable long-term corrosion protection to metallic structures. To address this problem, the coatings are generally modified to provide active corrosion protection.

A typical coating system for aircraft is composed of three coating layers namely, a polymeric top layer, an inhibitor containing primer layer and a passivating bottom layer. The schematic of aircraft paint system is shown in Figure 1. The topcoat which is generally an aircraft quality polyurethane paint serves as the main protective barrier against environmental influences such as extreme climates and ultra-violet rays. It also provides the aircraft acceptable optical and physical appearance (decoration and camouflage). A typical topcoat is formulated using a polyurethane resin. The second layer is primer which comprises of a pigmented organic resin matrix. Typical formulations consist of both chromated and non-chromated pigments enveloped in an epoxy resin. The thickness of the primer is typically 25 µm. The bottom most coating layer which is usually called conversion coating or pre-treatment layer is a very thin inorganic layer that provides corrosion protection and improved adhesion to the substrate. The thickness of this layer ranges from few nm to about 2 µm depending upon the nature of the coating.
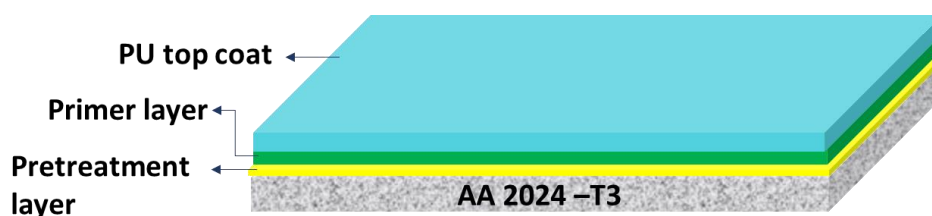

Figure 1 – Schematic representation of aircraft paint system.

Chromate conversion coating (CCC) is conventionally used as pre-treatment layer for AA 2024. Advantages of CCC includes excellent corrosion protection, economically feasible and ease of application, promotes adhesion etc. With all these functional features, the coating is banned because of its toxicity. Hexavalent chromium is a highly carcinogenic compound and hence it is a mandate to develop coatings or pre-treatments alternative to CCC. In this panorama, there have been several developments like permanganate, zinc phosphate, trivalent chromate, tungstate, vanadate, cerate and manganese based conversion coatings, sulfuric acid anodizing, boric-sulfuric acid and tartaric-sulfuric acid anodizing with suitable passivation and sealing [9-12]. In the last few decades, thin sol-gel films from hybrid metal alkoxide precursors are of growing interest as efficient pre-treatment layer to promote the adhesion between organic coatings and metal surfaces and also addressing environmental issues [13, 14].

A large amount of sol-gel research is based on silicon precursors because of their controlled and low reactivity, ease of handling and availability. Silanes have been widely studied since the first works of Plueddemann [15]. The chemistry of silanes and the mechanism of interaction of the molecules with the metallic substrate have been explained in the literature [16-18]. Hybrid coatings of 3-glycidoxypropyltrimethoxysilane (GPTMS) and Tetraethoxysilane (TEOS) are found to exhibit effective barrier nature against water and corrosive agents [19-22]. Incorporation of different inhibitors into the coatings has been reported to enhance the protection effectiveness of the organic-inorganic hybrid coatings [23-26]. There are other sol-gel systems with methacryloxypropyl triethoxysilane (MAPTES), and zirconium (IV) n-propoxide (TPOZ) reported for anticorrosion applications. They are prominent set of coatings studied that exhibit good anticorrosive performance with excellent adhesion and barrier nature on AA 2024 [27-29].

The objective of the present study was to develop alumina based sol-gel coatings for AA 2024 with improved corrosion protection properties and a low environmental impact. In particular, the present study aimed to investigate the behavior of the hitherto less explored silica-alumina hybrid coatings as sol-gel pre-treatment for AA 2024. Sol-gel films from silicon and aluminium alkoxides were

prepared and assessed for barrier property using electrochemical and exfoliation tests. Further, a comparative study on corrosion protection efficiency of the coatings with those containing cerium oxide nanoparticles as corrosion inhibitors has been carried out. Cerium oxide nanoparticles of different morphology were synthesized and characterized for shape, size and composition. The role of particle morphologies and chemical composition on surface protection ability of silica-alumina hybrid coatings has been elucidated.

2. Materials and methods

2.1 Materials

Unclad and Alclad AA 2024-T3 sheets of 1.2 mm thickness were procured from Alcoa, USA. Analytical grade chemicals, GPTMS, aluminium-tri-sec-butoxide (ASB) and ceria nanoparticles were obtained from Sigma, USA. Cerium (III) nitrate hexahydrate ($Ce(NO_3)_3.6H_2O$, 99%) and disodium hydrogen orthophosphate were obtained from Loba Chemie, India. Nitric acid, iso-propanol, ethanol, acetone and sodium hydroxide were from Merck, USA. All chemical reagents were of analytical grade and were used without any further purification. Lacquer was used to mask the uncoated area during salt spray studies and was procured from Shailtex Lubricants Industries, India. White epoxy paint along with thinner and hardener were procured from Southfield Paints Ltd., India. Water with resistivity of 18 MΩ cm was obtained from Milli Q water purification system and was used for all the preparations.

2.2 Preparation of hybrid sol and coating

- Silica-alumina sol

Silica-alumina hybrid sol was prepared from the individual sols of GPTMS and ASB. Sol containing GPTMS was prepared by mixing certain amount of GPTMS with ethanol and acidified H_2O (0.2 M HNO_3 as catalyst) for 2 h. The mole ratio of GPTMS: ethanol: H_2O was maintained at 1: 9: 2. The second sol containing ASB was prepared with EAA as the complexing agent. The mixture was stirred for about 30 min and then with acidified water for 1 h. The mole ratio of ASB, EAA and H_2O was 1: 2: 2. The two sols were mixed together and stirred for 2 h to obtain a hybrid sol of GPTMS and ASB. The pH of the prepared silica-alumina sol was ~ 4.5. The viscosity of the sol was in the range of 13-15 cP at a shear rate of 17 s^{-1}.

- Coating deposition

Dip coating technique was adopted to obtain uniform coatings on AA 2024 surface. The substrate was dipped into the sol followed by withdrawal of the substrate at a constant speed using a dip coater (SDC-2007C from Apex Instruments). The optimized dip coating parameters include dipping speed of 50 mm/min., withdrawal speed of 90 mm/min. and residence time of 1 min. After deposition, the coatings were cured at 25 °C for about 20 h and then heat treated at 100 °C for 2 h.

2.3 Characterization techniques used

The XRD patterns of powder samples were recorded using Bruker D8 Advance diffractometer with Ni filtered Cu Kα (λ=1.5406 Å) as the source at 35 kV, 10 mA. Crystallite size of particles was determined using Scherrer equation. Morphology of the samples was examined using field emission scanning electron microscopy (FESEM) Carl Zeiss, model Supra 40VP with a Gemini column. Powder samples were prepared by dispersing it in a solvent by ultrasonication for 15 – 20 min and drop casted on a polished brass stud. Sol-gel coatings along with the substrates were cut into small pieces and placed directly on the sample holder using carbon tape. Transmission electron microscopy (TEM) was carried out using JEOL-JEM 2100F and Technai G2 F-30 transmission electron microscopes. Few drops of the sonicated powder sample in a solvent were placed on a copper mesh for TEM. Leica Application suite microscope software was used for image analysis. X-ray photoelectron spectroscopy (XPS) studies were carried out (SPECS spectrometer, Germany) using non-monochromatic Al Kα radiation (1486.6 eV) as X-ray source operated at 150 W (12 kV and 12.5 mA). The binding energies reported are referenced with C1s peak at 284.6 eV. Casa XPS program was employed for curve-fitting all core level spectra into several components with Gaussian−Lorentzian peaks after Shirley background subtraction.

The surface roughness of the sol–gel coatings were measured using a 3D profilometer from AEP technology, model NanoMap 500 LS were used. The coating thickness was measured using digimatic micrometer, Model Mitutoyo 293–805 and cross-sectional FESEM images. Hardness and scratch resistance of the coating was measured using pencil hardness tester, model Elcometer 501, according to the ISO 15184 standard. Adhesion between the coating layer and the substrate was assessed by tape-peel-off method according to the ASTM D3359 standard test method, using cross hatch cutter, model Elcometer 107. The viscosity of the prepared sol was measured using Brookfield DV-III ultra-programmable rheometer. The pH of the sols was measured using a pH meter, model Cyberscan 510.

Electrochemical impedance spectroscopy (EIS) measurements were carried out using using CHI604D electrochemical workstation. The tests were carried out in 3.5 wt. % (0.6 M) NaCl solution using a conventional three electrode cell. Sol-gel coated coupon with 1 cm^2 active area was used as the working electrode, platinum foil as the counter electrode and standard calomel electrode (SCE) connected to a luggin capillary as the reference electrode. EIS data was obtained over the frequency domain of 100 kHz to 10 mHz by applying a 10 mV sinusoidal wave. The acquired data are curve fitted and analyzed using ZSimpwin program. Industry standard corrosion tests were conducted at accelerated testing conditions in a salt spray chamber, where the panels were exposed to highly corrosive conditions (5 % NaCl solution) more aggressive than the environment at which the material is intended to be used. The tests were conducted in salt spray chamber, model Ascott Sxp 120 according to standard ASTM B117.

3. Results and Discussion

3.1 Surface preparation for coating deposition

Surface preparation is an important step for subsequent coating deposition and corrosion protection. The native oxide must be suitably modified such that it holds the coating layers without causing any adverse effects. The alloy sheets were cut into 25 × 15 mm^2 pieces and used unabraded. The nominal composition of unclad AA 2024 was found to be Al-89.44 %, Cu-5.82 %, Mg-3.68 %, Si-0.28 %, Ti-0.44 % and Zn-0.35 %. Five types of surface treatments were studied namely Acetone degreasing, Mechanical grinding and polishing with 1μm alumina, chemical etching in alkaline and acid solutions and treating with a cleaning liquid named Pyro AluSolv-175. The samples then thoroughly washed with running water and rinsed in distilled water. They were completely dried at room temperature in a desiccator for about 15 min for the water to evaporate and then were immediately coated with a standard sol. They were cured and subjected to salt spray test. As seen in Figure 2, chemically etched surface remained bright and corrosion free for longer duration compared to other samples. Based on this observation, chemical etching was chosen as the surface preparation process in the present study.
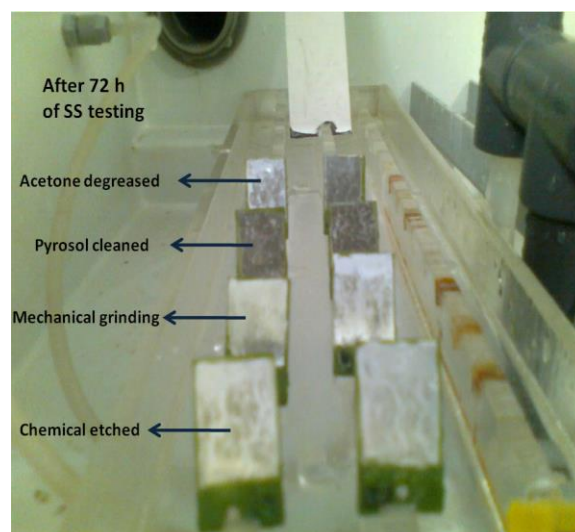

Figure 2 – Salt spray test of samples with different surface preparation procedures.

3.2 Corrosion performance of silica-alumina hybrid coating

Silica-alumina hybrid sols in different mole ratios of GPTMS and ASB precursors were prepared. The coatings from these sols were tested for their intactness by immersing in corrosive electrolyte (3.5 % NaCl) as shown in Figure 3. Coatings from sol containing GPTMS: ASB mole ratios 1:1 and 3:1 developed several pits with white corrosion deposits on the surface observed in 3-4 days. Microscopic images of coatings with GP-AB in 1:1 mole ratio showed several tiny cracks on the surface while coatings with GP-AB in 3:1 mole ratio showed pin hole like formation on the surface. On the other hand, surfaces of coatings with GP-AB in 2:1 ratio were relatively smooth (Figure 4). The porosity of the coatings was determined from the FESEM images using image analysis software. Surface porosity of GP-AB coatings with mole ratios 1:1, 2:1 and 3:1, in terms of area percentage are estimated to be 6.9, 0.03 and 2.2, respectively. Thus, it appears that the presence of tiny cracks and defects in the coatings are responsible for penetration of NaCl solution and subsequent corrosion on AA 2024.

Figure 3 – Photograph of silica-alumina coatings with varied GPTMS and ASB mole ratio, immersed in NaCl solution
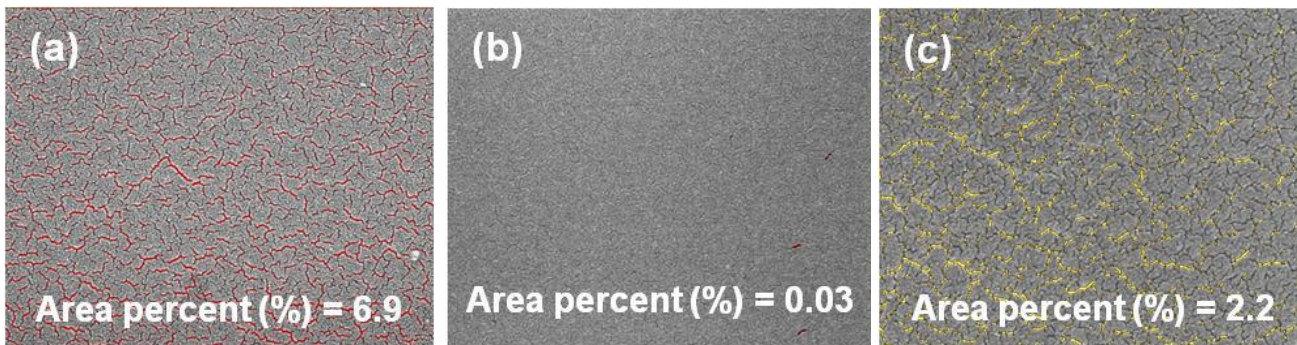

Figure 4 – Surface porosity of silica-alumina coatings with mole ratios (a) 1:1, (b) 2:1 and (c) 3:1, in terms of percentage area.

It was evident that coatings obtained from silica and alumina precursors in the mole ratio 2:1 showed good barrier property against the ingress of corrosive electrolyte with minimum defects in the coatings. GP-AB 2:1 withstood NaCl immersion for longer duration without any significant pitting. Hence, all further studies, characterization and inhibitor addition were carried out with these coatings. The surface microstructural image of sol–gel hybrid coating (2:1) is shown in Figure 5a. The coating was found to be very uniform and defect free without any cracks. Typical photograph of the prepared coating is shown in Figure 5b. Thickness of the coating was determined using a thickness gauge and a roughness profilometer. Step-up profile obtained on the coating on moving the stylus tip from uncoated region to the coated region is shown in Figure 5c. Thickness of the coating was around 2.3±0.1 µm.
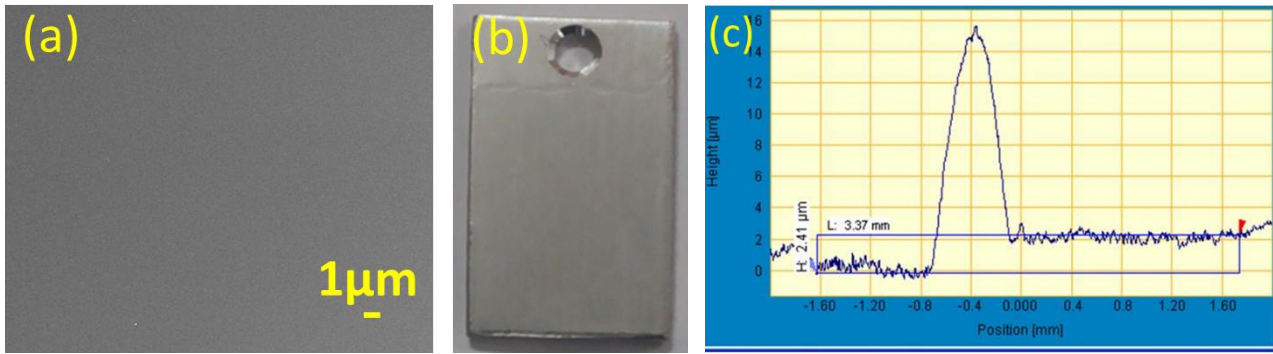
Figure 5 – (a) Microscopic image, (b) photographic image and (c) thickness determination of 2:1 silica-alumina coating

The average roughness of the coatings was around 160 nm (Figure 6a). The coated samples showed excellent scratch resistance. Pencil with the highest hardness of 9H was unable to make a cut in the coatings. Thus, the coatings exhibited a pencil hardness of > 9H. They also exhibited very good adhesion with the substrate. The coatings remained intact and there was no spallation at the edges of the cross-hatch cut lattice showing the highest rating of 5B. Figure 6b shows a typical image of cross hatch cut of the coated sample after the adhesion test. This confirmed the mechanical properties of silica-alumina hybrid coatings was good.
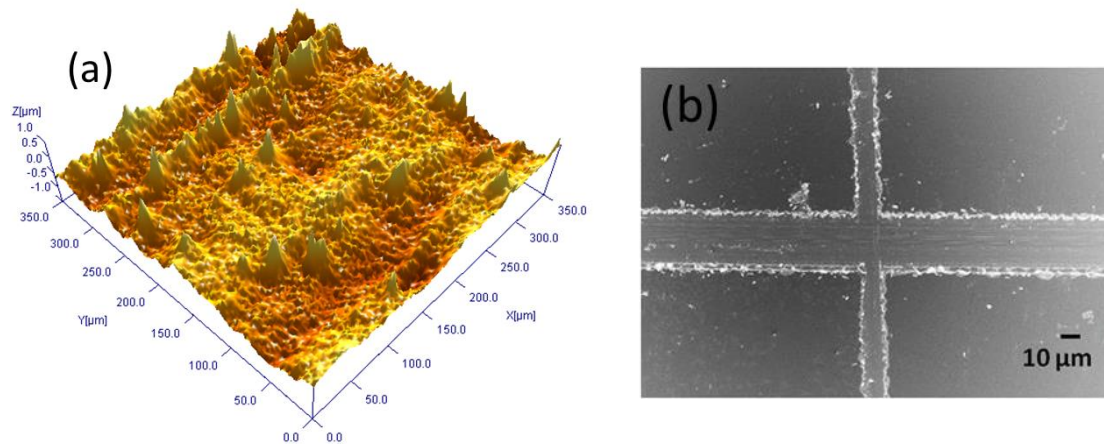
Figure 6 – (a) Surface roughness map and (b) cross hatch cut image of the coating

To impart active corrosion protection, cerium nitrate and ceria nanoparticles of different morphologies were used as corrosion inhibitors in the sol-gel coatings [30-33]. They were deposited on AA 2024-T3 substrate in a similar fashion described earlier. The coatings did not change their appearance and its physical properties due to cerium nitrate addition. The presence of cerium ions in the sol-gel matrix in the coating was confirmed through XPS studies by recording Ce-3d core level spectra. Since the concentration of cerium nitrate added is in very low concentration (2.5-5.0 mM), weak peaks at 885 and 904.5 eV which correspond to the $3d_{5/2}$ and $3d_{3/2}$ peaks of cerium ions were observed.

To assess the corrosion inhibition performance, the coated samples were tested to gain insight into their barrier properties and corrosion inhibition ability. The impedance data obtained for the cerium nitrate modified coatings are displayed as Bode plot (Figure 7). The impedance modulus values at the low frequency region of Bode plot can be compared to understand the corrosion protection ability of the coating. A high value corresponds to good protection. It is observed that cerium nitrate modified coatings provided corrosion protection to the substrate compared to bare uncoated surface [30]. However, the corrosion protection ability gradually falls with immersion time in NaCl. Continued immersion leads to electrolyte ingression through the pores in the coating leading to corrosion. The marginal improvement in the low frequency impedance observed at 240 h immersion may be due to filling of pores by corrosion products.
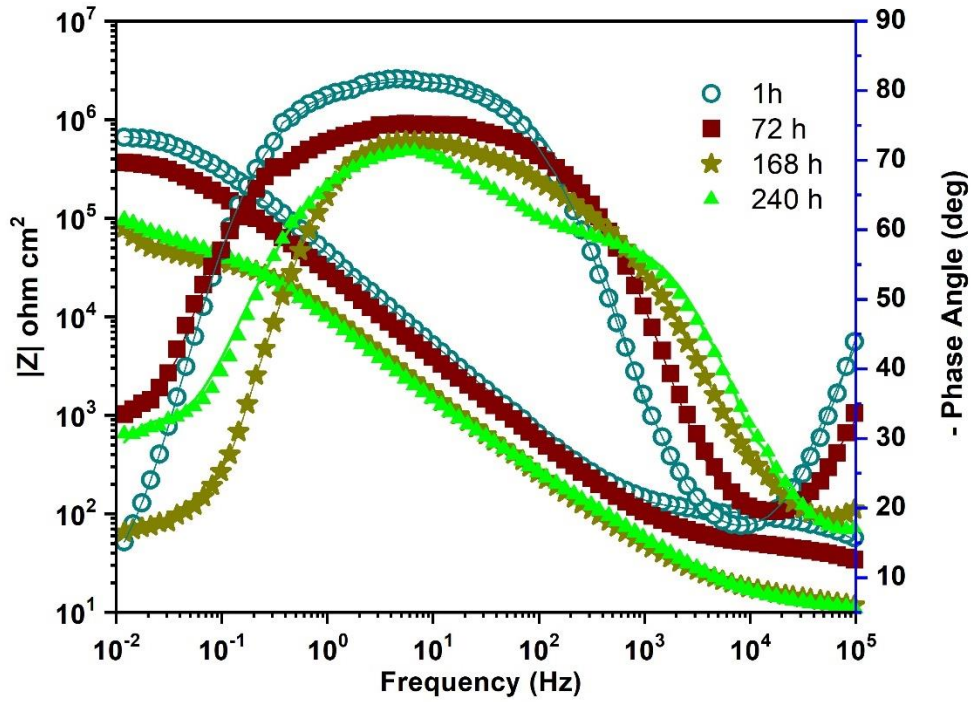
Figure 7 – Bode plot for 2.5 mM cerium nitrate modified silica-alumina coatings on AA 2024 at different immersion times in 3.5 % NaCl.

The obtained EIS curves were fitted with two and three-time constant electrochemical equivalent circuits (EECs) as depicted in Figure 8. The lines on the data points represent the fitted data. The substrate-coating system is assumed to consist of three interfaces. The first one is between sol–gel coating and the electrolyte. The second is an oxide layer which includes the natural alumina layer of the substrate and the oxide linkages formed between the Al-OH groups of substrates and the Si-OH or/and Al-OH groups of the hybrid sol. This interaction leads to the formation of Al-O-Si bonds or/and Al-O-Al bonds. The third interface is the metal surface on which corrosion happens. The impedance parameters obtained after fitting the data with EECs are given in Table 1. Use of constant phase element (CPE) is justified due to surface roughness, inhomogeneous reaction rates on the surface, or varying thickness or composition of a coating.
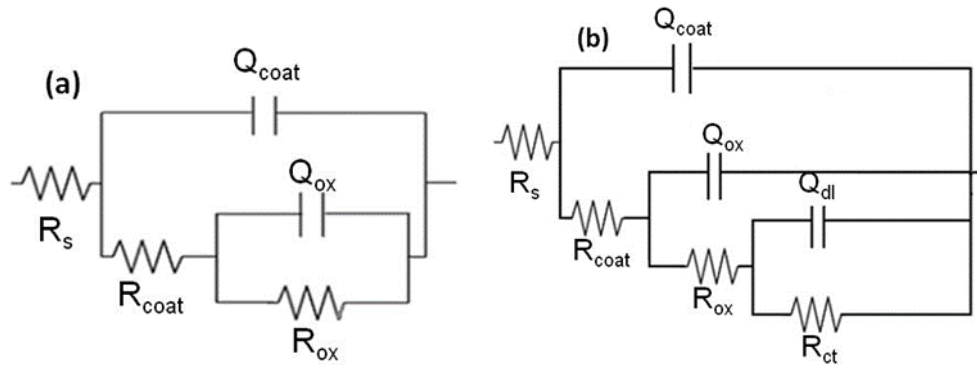

Figure 8 – Electrochemical equivalent circuits (EECs) used for samples at (a) initial immersion times showing two time constants and (b) Prolonged immersions exhibiting three time constants.

From the values in the table, it is seen that there is significant reduction in the R_{coat} and R_{ox} values upon exposure to NaCl. A third time constant is seen to appear after 168 h of immersion. The R_{ox} values reduce from 725 kΩ cm^2 to 51.6 kΩ cm^2 after 168 h of immersion. The coating capacitance also increases by about an order of magnitude. This is a clear indication of water uptake in to the coating leading to coating deterioration. Thus, when compared to cerium nitrate unmodified coatings, 2.5 mM cerium nitrate modified coatings do not show any degradation and hence it is likely that the cerium nitrate concentration can be further increased to enhance the corrosion inhibition property rendered by the coating to the surface.

Table 1 – EIS data for 2.5 mM cerium nitrate modified coatings obtained by fitting with the EECs

Immersion time (h)	Q_{coat} (μSs^n /cm^2)	n_{coat}	R_{coat} (kΩ cm^2)	Q_{ox} (μSs^n /cm^2)	n_{ox}	R_{ox} (kΩ cm^2)	Q_{dl} (μSs^n /cm^2)	n_{dl}	R_{ct} (kΩ cm^2)
1	0.29 ±0.01	0.8 ±0.01	0.107 ±0.06	3.92 ±0.02	0.92 ±0.01	725.7 ±40	-	-	-
72	1.24 ±0.12	0.7 ±0.02	0.055 ±0.02	6.56 ±0.34	0.86 ±0.02	518 ±16	-	-	-
168	1.26 ±0.23	0.76 ±0.02	0.015 ±0.32	18.6 ±11	0.81 ±0.01	51.6 ±0.02	417 ±15	0.95 ±0.02	46.4 ±1.6
240	18.06 ±0.4	0.78 ±0.04	0.56 ±0.03	4.13 ±0.08	0.93 ±0.01	73.3 ±0.2	215 ±19	0.98 ±0.02	67.4 ±2.2

It has been reported that cerium nitrate inhibitor migrates to the corrosive spots, precipitates in the alkaline pH conditions and thus protects the surface [34-36]. Recently, Uhart et al. [37] have monitored the location of cerium on AA 2024 T3 substrate with scanning auger microscopic survey and observed that cerium tends to move in a short time, towards the active spots leaving the surrounding coating almost free of inhibitor content. In the present study, XPS analysis has been carried out to confirm the migration of cerium ions into the surface active sites. Sol-gel coating modified with 5 mM cerium nitrate is used for this purpose. A coated sample of size 6 mm x 6 mm is taken, and multiple crosshatch cuts are deliberately made with a sharp needle. Corrosion process is initiated on the surface by placing 2 drops of 3.5 % NaCl solution and the sample is left at 25 °C in a petridish for 4 days. Drops of NaCl solution are added on to the surface periodically to compensate for evaporation. The survey spectra and Ce 3d spectral regions obtained before and after NaCl exposure are shown in Figure 9a and 9b, respectively. The area under the Ce 3d and Si 2p peaks are taken to estimate relative concentrations of Ce and Si and to subsequently find out the outward migration of Ce. Since Al forms part of both the substrate and coating, it is not included in the estimation. It is observed that the concentration of Ce increases from 1 at. % before NaCl exposure to 2.7 at. % after NaCl immersions, thus providing strong evidence to the above hypothesis.
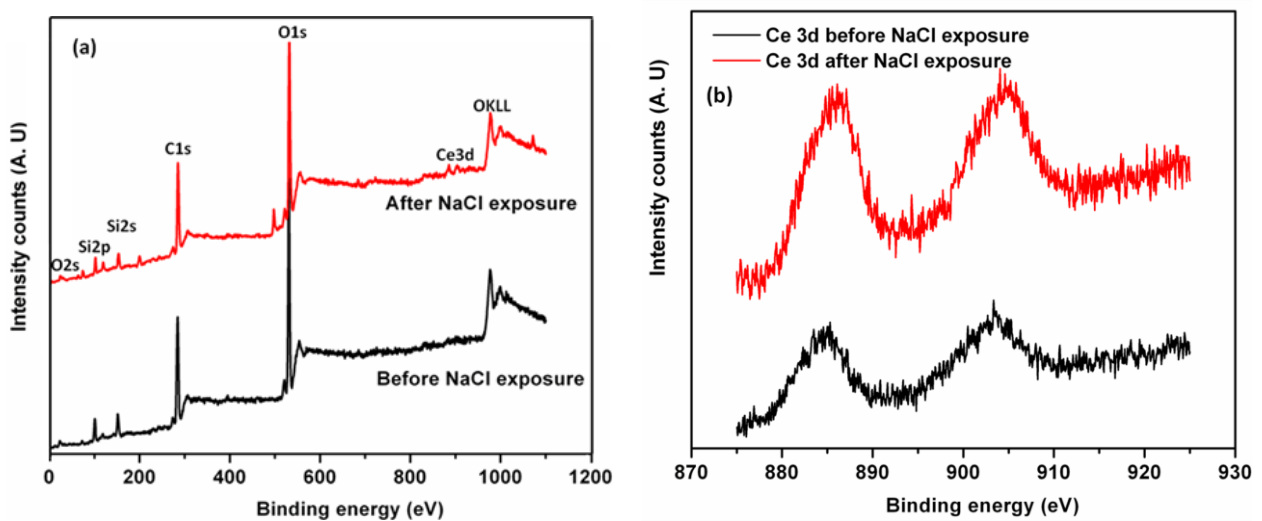

Figure 9 – XPS spectra of the cerium nitrate modified silica-alumina coating before and after NaCl exposure, (a) survey spectra (b) Ce 3d core level spectral region.

Cerium nanoparticles with various shapes and sizes were used as corrosion inhibitors in-lieu of cerium nitrate in silica-alumina sol-gel coating [31-33]. It was found that cerium oxide nanofibers incorporated sol-gel coating exhibited better corrosion resistance than the coating containing

spherical and cubic shaped ceria nanoparticles. The silica-alumina sol-gel coating was examined for its compatibility with conventional strontium chromate loaded primer layer. This test particularly aimed at testing the adhesion of the sol-gel based pretreatment layer with the substrate as well as the subsequent top layers. This is a very critical issue since the long term corrosion protection ability of the coating depends on how good the coatings are adherent to each other without leading to any blisters or peel-offs on prolonged exposure to corrosive environments. Samples were prepared under identical conditions as per regular procedure. The sol-gel coated surface was coated with yellow primer. For comparison, a CCC treated surface with yellow primer layer was also kept in the salt spray. Scribes were made deliberately on the both the samples and were tested with 5 % NaCl solution as per ASTM standard B 117. The photographs of the samples recorded after regular intervals of time are shown in Figure 10. It is observed that the silica-alumina hybrid coatings had very good adhesion with the top primer layer and led to no blistering or peeling off the paint. The results were almost comparable with conventional CCC.

Coating details	Sol-gel coating with yellow primer-sample 1	CCC coating with yellow primer - sample 2
Before testing		
After 168 h of salt spray test		
After 336 h of salt spray test		

Figure 10 – Photographs showing good compatibility of silica-alumina sol-gel pretreatment layer with yellow primer vis-à-vis CCC pretreatment layer with yellow primer.

Conclusions

In the present study, the less explored silica–alumina hybrid sol-gel coatings were developed and studied for their anticorrosion properties using electrochemical techniques and industry-standard tests. The corrosion resistance of the developed coatings containing cerium nitrate, ceria nanoparticles (sphere, cubes) and cerium oxide nanofibers has been evaluated. The coatings have shown corrosion resistance at par with the conventional chromate conversion coatings. The coatings have also exhibited compatibility with the top primer layers as evident from the salt-spray test. The current study has shown that silica-alumina hybrid sol-gel coating containing Ce-based corrosion inhibitors as a propitious alternate to CCC for aircraft paint coating system.

Contact Author Email Address

R.V. Lakshmi : lakshmi_rv@nal.res.in

Copyright Statement

Acknowledgements

References

[1] Starke Jr E.A and Staley J.T, Application of modern aluminum alloys to aircraft**.** *Progress in Aerospace Science,* Vol. 32, pp 131-172, 1996.

[2] Buchheit R.G, Grant R.P, Hlava P.F, McKenzie B and Zender G.L, Local dissolution phenomena associated with S phase (Al$_2$CuMg) particles in aluminum alloy 2024-T3. *Journal of Electrochemical Society*, Vol. 144, pp. 2621-2628, 1997.

[3] Zhu D and van Ooij W.J. Corrosion protection of AA 2024-T3 by bis-[3-(triethoxysilyl)propyl]tetrasulfide in neutral sodium chloride solution. Part 1: corrosion of AA 2024-T3.*Corrosion Science,* Vol. 45, No. 10, pp 2163–2175, 2003.

[4] P. Campestrini, E. P. M. van Westing, H. W. van Rooijen, J. H. W. de Wit, Relation between microstructural aspects of AA2024 and its corrosion behaviour investigated using AFM scanning potential technique. *Corrosion Science, Vol.* 42, No. 10, pp**.** 1853-186, 2000.

[5] Hughes AE, MacRae C, Wilson N, Torpy A, Muster T.H and Glenn A.M. Sheet AA2024-T3: a new investigation of microstructure and composition, *Surface and Interface Analysis*, Vol. 42 , No. 4, pp 334-338, 2010.

[6] Hughes A.E, Parvizi R and Forsyth M. Microstructure and corrosion of AA2024.*Corrosion Reviews*, Vol. 33, pp 1-30, 2015.

[7] Guillaumin V and Mankowski G. Localized corrosion of 2024 T351 aluminium alloy in chloride media. *Corrosion Science*, Vol. 41, No.3, pp 421-438, 1998.

[8] Obispo H.M, Murr L.E, Arrowood R.M and Trillo E.A. Copper deposition during the corrosion of aluminum alloy 2024 in sodium chloride solutions, *Journal of Materials Science,* Vol. 35, pp. 3479–3495, 2000.

[9] Danilidis I, Hunter J, Scamans G.M and Sykes J.M. Effects of inorganic additions on the performance of manganese-based conversion treatments. *Corrosion Science, Vol.* 49, No. 3, pp.1559–1569, 2007.

[10] Yoganandan G, Balaraju J.N and Grips V.K.W. The surface and electrochemical analysis of permanganate based conversion coating on alclad and unclad 2024 alloy. *Applied Surface Science*, Vol. 258, pp 8880– 8888, 2012.

[11] Twite R.L and Bierwagen G.P. Review of alternatives to chromate for corrosion protection of aluminum aerospace alloys*. Progress in Organic Coatings,* Vol. 33, No.2, pp 91–100, 1998.

[12] Kuznetsov B, Serdechnova M, Tedim J, Starykevich M, Kallip S, Oliveira M.P, Hack T, Nixon S, Ferreirac M.G. S,

Zheludkevich M.L, Sealing of tartaric sulfuric (TSA) anodized AA2024 with nanostructured LDH layers. *RSC Advances,* Vol. 6, pp 13942-13952, 2016.

[13] Wang D and Bierwagen G.P, Sol–gel coatings on metals for corrosion protection. *Progress in Organic Coatings*. Vol. 64, No.4, pp 327-338, 2009.

[14] Figueira R.B, Silva C.J.R, Pereira E.V. Organic–inorganic hybrid sol–gel coatings for metal corrosion protection: a review of recent progress. *Journal of Coatings and Technology Research,* Vol.12, pp 1-35, 2015.

[15] Pluddemann E.P, Adhesion through silane coupling agents, *Journal of Adhesion*, Vol.2, pp. 184-201, 1970.

[16] Pluddemann E.P. *Silane coupling agents*, 2nd ed., Plenum Press,1990.

[17] Pu Z, van Ooij W.J and Mark J.E. Hydrolysis kinetics and stability of bis(triethoxysilyl)ethane in water-ethanol solution by FTIR spectroscopy. *Journal of Adhesion Science and Technology,* Vol.11, No.1, pp 29-47, 1997.

[18] Montemor M.F, Simões A.M, Ferreira M.G.S, Williams B and Edwards H, The corrosion performance of organosilane based pre-treatments for coatings on galvanised steel. *Progress in Organic Coatings*. Vol. 38, No.1, pp 17-26, 2000.

[19] Tiringer U, Milosev I, Duran A and Castro Y. Hybrid sol–gel coatings based on GPTMS/TEOS containing colloidal SiO_2 and cerium nitrate for increasing corrosion protection of aluminium alloy 7075-T6. *Journal of Sol-Gel Science and Technology*, Vol. 85, pp.546-557, 2018.

[20] Wu K.H, Chao C.M, Yeh T.F and Chang T.C. Thermal stability and corrosion resistance of polysiloxane coatings on 2024-T3 and 6061-T6 aluminum alloy. *Surface and Coatings Technology*, Vol. 201, No.12, pp. 5782–5788, 2007.

[21] Tavandashti N.P, Sanjabi S, Shahrabi T, Corrosion protection evaluation of silica/epoxy hybrid nanocomposite coatings to AA2024.. *Progress in Organic Coatings*, Vol. 65, No.2, pp 182–186, 2009.

[22] Kozhukharov S, Kozhukharov V, Schem M, Aslan M, Wittmar M, Wittmar A and Veith M, Protective ability of hybrid nano-composite coatings with cerium sulphate as inhibitor against corrosion of AA2024 aluminium alloy. *Progress in Organic Coatings*, Vol. 73, pp. 95–103, 2012.

[23] Lampke T, Darwich S, Nickel D and Wielage B. Development and characterization of sol-gel composite coatings on aluminum alloys for corrosion protection. *Materialwissenschaft und Werkstofftechnik.* Vol. 39, pp 914–919, 2008.

[24] E. Roussi, A. Tsetsekou, A. Skarmoutsou, C.A. Charitidis, A. Karantonis, Anticorrosion and nanomechanical performance of hybrid organo-silicate coatings integrating corrosion inhibitors. *Surface and Coatings Technology*. Vol. 232, pp. 131–141, 2013.

[25] Naderi R, Fedel M, Deflorian F, Poelman M and Olivier M. Synergistic effect of clay nanoparticles and cerium component on the corrosion behavior of eco-friendly silane sol–gel layer applied on pure aluminum. *Surface and Coatings Technology*, Vol. 224, pp. 93-100, 2013.

[26] Capelossi V.R, Poelman M, Recloux I, Hernandez R.P.B, de Melo H.G and Olivier M.G. Corrosion protection of clad 2024 aluminum alloy anodized in tartaric-sulfuric acid bath and protected with hybrid sol–gel coating. *Electrochimica Acta,* Vol. 124, pp. 69-79, 2014.

[27] Poznyak S.K, Zheludkevich M.L, Raps D, Gammel F, Yasakau K.A and. Ferreira M.G.S, Preparation and corrosion protective properties of nanostructured titania-containing hybrid sol–gel coatings on AA2024. *Progress in Organic Coatings*, Vol. 62, No.2, pp. 226–235, 2008.

[28] Yasakau K.A, Zheludkevich M.L, Karavai O.V and Ferreira M.G.S., Influence of inhibitor addition on the corrosion protection performance of sol-gel coatings on AA2024. *Progress in Organic Coatings*, Vol. 63, No.3. pp. 352–36, 2008.

[29] Alvarez P, Collazo A, Covelo A, Novoa X.R and Perez C. The electrochemical behaviour of sol–gel hybrid coatings applied on AA2024-T3 alloy: Effect of the metallic surface treatment. *Progress in Organic Coatings*, Vol. 69, No.2, pp. 175–183, 2010.

[30] Lakshmi R.V, Aruna S.T, Anandan C, Parthasarathi Bera and Sampath S. EIS and XPS studies on the self-healing properties of Ce-modified silica-alumina hybrid coatings: Evidence for Ce(III) migration. *Surface and Coatings Technology*, Vol. 309, pp. 363-370, 2017.

[31] Lakshmi R.V, Aruna S.T and Sampath, S. Ceria nanoparticles vis-à-vis cerium nitrate as corrosion inhibitors for silica-alumina hybrid sol-gel coating. *Applied Surface Science*, Vol. 393, pp. 397-404, 2016.

[32] Lakshmi R.V, Sampath S and Aruna S.T. Silica-alumina based sol-gel coating containing cerium oxide nanofibers as a potent alternative to conversion coating for AA2024 alloy, *Surface and Coatings Technology*, Vol. 411, pp. 127007, 2021.

[33] Lakshmi R.V, Kamalesh Pal, Tapas Kumar Mandal and Aruna S.T. Multifunctional properties of ceria nanocubes synthesized by a hydrothermal method, *Bulletin of Materials Science*, Vol. 42, pp 21, 2019.

[34] Waters D.N and Henty M.S. Raman spectra of aqueous solutions of hydrolysed aluminium(III) salts, *Journal of the Chemical Society, Dalton Transactions*, pp. 243-245, 1977.

[35] E. Campazzi, C. Druez, S. de Monredon-Senani, Villatte, 22nd 3AF colloquium, Paris, November 27−28, 2007

[36] Crossland A.C, Thompson G.E, Skeldon P, Wood G.C, Smith C.J.E, Habazaki H and Shimizu K. Anodic oxidation of Al-Ce alloys and inhibitive behaviour of cerium species. Corrosion Science, Vol. 40, No.6, pp. 871-885, 1998.

[37] Uhart A, Ledeuil J.B, Gonbeau D, Dupin J.C, Bonino J.P, Ansart F, Esteban J, An Auger and XPS survey of cerium active corrosion protection for AA2024-T3 aluminum alloy. *Applied Surface Science*, Vol. 390 pp. 751-759, 2016.